

# Paracrystalline Lattice Distortion in the Near-Surface Region of Melt-Crystallized Polyethylene Films Evaluated by Synchrotron-Sourced Grazing-Incidence X-ray Diffraction

Hirohiko Yakabe,<sup>†</sup> Sono Sasaki,<sup>†</sup> Osami Sakata,<sup>‡</sup> Atsushi Takahara,<sup>§</sup> and Tisato Kajiyama<sup>\*,†</sup>

Department of Applied Chemistry, Graduate School of Engineering, Kyushu University, Fukuoka 812-8581, Japan; Japan Synchrotron Radiation Research Institute, Sayo, Hyogo 679-5198, Japan; and Institute for Materials Chemistry and Engineering, Kyushu University, Fukuoka 812-8581, Japan

Received April 24, 2003

Revised Manuscript Received June 20, 2003

Physical properties of polymeric materials such as adhesion and friction relate to molecular aggregation structure in the material's surface. However, the surface of crystalline polymers has been studied mainly from morphological and chemical points of view. In the case of polyethylene (PE), a typical example of crystalline polymers, the surface morphology of its solid films was visualized in the lamellar scale by atomic force microscopy and transmission electron microscopy.<sup>1–3</sup> However, the crystal structure at the surface of PE films has not yet been clarified. Clarification of the crystal structure on the film surface is quite important for understanding the surface property from the molecular level. A grazing incidence X-ray diffraction (GIXD) using evanescent X-rays has recently been applied for evaluating chain-packing structure and chain orientation in the near-surface region of crystalline polymers.<sup>4–8</sup> In this study, the dimension and distortion of the crystal lattice in the near-surface region of melt-crystallized PE films were investigated by synchrotron-sourced GIXD measurements.

A high-density polyethylene (HDPE, MI = 14, Mitsui Chemicals, Inc.) was used as a sample. Films with a thickness of ca. 400 nm were prepared on the crystallographic (110) plane of silicon substrates from a 1.0 wt % *p*-xylene solution of HDPE by a dip-coating method under a nitrogen atmosphere. The size of silicon substrates used was 1 in. in diameter and 3 mm in thickness. The thus-prepared PE films were melted at ca. 443 K and then isothermally crystallized at  $T_c$  = 378, 383, 388, and 393 K for 24 h. The crystal structure in the near-surface region of the films was investigated by in-plane measurements of grazing-incidence wide-angle X-ray diffraction (GIXD). GIXD measurements were carried out on the films at 300 K with a six-axis diffractometer installed at a BL-13XU beamline of SPring-8 (Japan Synchrotron Radiation Research Institute, Hyogo, Japan).<sup>9</sup> The wavelength,  $\lambda$ , of monochromatized incident X-rays used in this study was 0.1285 or 0.1280 nm. The beam size at incident slits was

0.10 and 0.06 mm in the normal and parallel directions to the ground, respectively. Figure 1 shows the schematic geometry of the in-plane GIXD measurement. In the experiments, the surface of the sample was normal to the ground. The scattering vector  $q$  is almost parallel to the surface for the grazing angle of incident X-rays,  $\alpha_i$ . At a  $\alpha_i$  equal to the critical angle,  $\alpha_c$ , incident X-rays undergo total external reflection and penetrate into a sample as evanescent waves. With a decrease in  $\alpha_i$  smaller than  $\alpha_c$ , the penetration depth of evanescent X-rays from the surface decreases from several micrometers to nanometers. The  $\alpha_c$  of HDPE is 0.1257° for  $\lambda$  = 0.1285 nm and 0.1253° for  $\lambda$  = 0.1280 nm. Therefore, the reflection profiles coming from the surface and bulk regions of the HDPE films were measured at the  $\alpha_i$  of 0.11° and 0.20°, respectively. Bragg diffraction from crystallographic planes normal to the surface and amorphous scattering were detected at the takeoff angle,  $\alpha_f$ , of 0.22° and 0.40° with a scintillation counter (SC) scanned in the in-plane direction. A soler slit with an acceptance angle of 0.3° was placed before the SC. The data collection time was 3 s per step, and the angular interval between steps was 0.05°. A sample cell purged with helium gas was used to prevent HDPE films from oxidation. Broadening in the width of the profiles caused by angular divergence of the incident X-rays was negligibly small, as evaluated using reflections from silicon crystals. Data correction was performed with respect to the background scattering and the intensity decay of incident X-rays during measurements. Surface morphology and crystallographic orientation were evaluated for the films by atomic force microscopic observations and GIXD measurements in the laboratory. On the basis of these data, it was found that the films were crystallographically isotropic in the parallel direction to the film surface but anisotropic in the perpendicular direction. This is due to spherulites that grew two-dimensionally filling the films. The details of film characterization will be described in a future paper.

Parts a and b of Figure 2 show in-plane GIXD profiles measured at  $\alpha_i$  = 0.11° and 0.20°, respectively, for a HDPE film crystallized isothermally at 383 K from the melt on a silicon substrate. The  $\lambda$  of the incident X-rays was 0.1285 nm, and the ideal penetration depth of the X-rays from the surface at  $\alpha_i$  = 0.11° was ca. 10 nm.<sup>10</sup> Figure 2a is a surface-sensitive profile of the film, and Figure 2b is a bulk-sensitive one. Overlapping peaks were separated by the least-squares fitting with Lorentzian and Gaussian functions as shown by the solid line in Figure 2. It is well-known that HDPE forms an orthorhombic crystal structure (the space group  $Pnam$ ).<sup>11</sup> Peaks in a  $2\theta_{\text{in-plane}}$  range of 8–57° were assigned reasonably to the reflections from the orthorhombic crystal. Profiles similar to Figure 2 were measured for HDPE films crystallized at  $T_c$  = 378, 388, and 393 K. Lattice constants  $a$ ,  $b$ , and  $c$  of the orthorhombic unit cell of the HDPE were calculated from the  $2\theta_{\text{in-plane}}$  angles of the reflection peaks. Figure 3 shows the crystallization temperature dependence of the lattice constants  $a$ ,  $b$ , and  $c$  in the near-surface and bulk regions of the HDPE films. The  $a$  and  $b$  axial lengths of the orthorhombic unit cell were shorter in the near-surface region than in the bulk region, whereas the  $c$  axis was almost the same length in both the regions.

<sup>†</sup> Department of Applied Chemistry, Graduate School of Engineering, Kyushu University.

<sup>‡</sup> Japan Synchrotron Radiation Research Institute.

<sup>§</sup> Institute for Materials Chemistry and Engineering, Kyushu University.

\* To whom correspondence should be addressed. E-mail: kajiyama@cstf.kyushu-u.ac.jp.

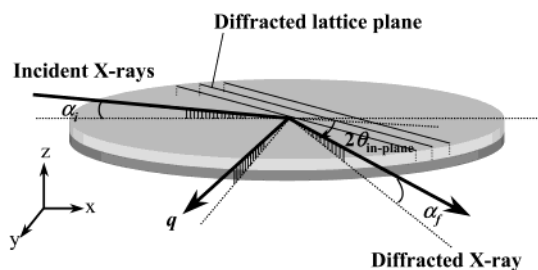


**Figure 1.** Schematic geometry of the in-plane GIXD measurement.

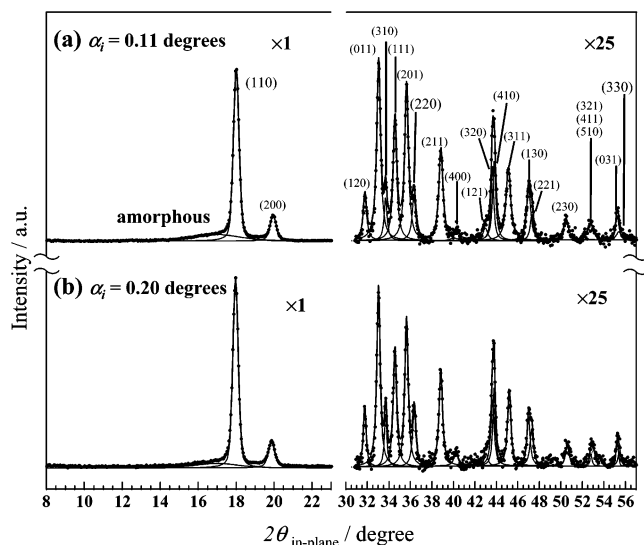


**Figure 2.** In-plane GIXD profiles measured at  $\alpha_i = 0.11^\circ$  (a) and  $0.20^\circ$  (b) for a HDPE film crystallized isothermally at 383 K from the melt. The  $\lambda$  of incident X-rays was 0.1285 nm.

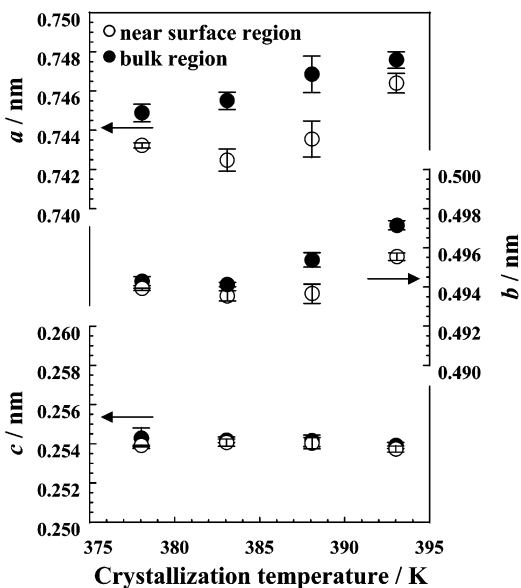


**Figure 3.** Crystallization temperature dependence of the lattice constants  $a$ ,  $b$ , and  $c$  of the orthorhombic unit cell in the near-surface and the bulk regions of the HDPE films:  $\circ$ , near-surface region;  $\bullet$ , bulk region. Error bars indicate estimated errors in data analysis.

Therefore, it was implied that the crystal density in the near-surface region is higher than that in the bulk region in a  $T_c$  range of 378–393 K. With an increase in  $T_c$ , the  $a$  and  $b$  increased in both of the regions. However, the  $c$  axial length showed little change. It is

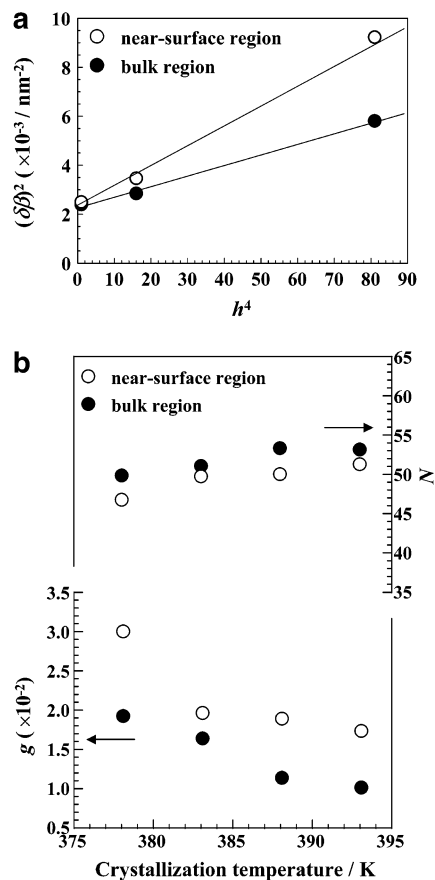


**Figure 4.** (a)  $(\delta\beta)^2$  plot as a function of  $h^4$  for the (110), (220), and (330) reflections of the HDPE film crystallized isothermally at  $T_c = 383$  K from the melt. (b) Crystallization temperature dependence of the  $g$  and  $N$  for the HDPE films crystallized isothermally at  $T_c = 378, 383, 388$ , and  $393$  K from the melt.  $\circ$ , near-surface region;  $\bullet$ , bulk region.

reasonable to consider that the  $c$  axis of the orthorhombic crystal lattice is dimensionally stable in the films because it is parallel to the chain axis.<sup>12</sup>

The distortion of crystal lattice in the in-plane direction was estimated on the basis of the paracrystalline theory proposed by Hosemann.<sup>13–15</sup> In the paracrystalline lattice model, the lattice vectors of adjacent unit cells vary in magnitude and direction due to large displacement of lattice points from their ideal positions, which results in a loss of the long-range crystallographic order. On the assumption that the coordination statistics distribution function for the paracrystalline lattice model is in the form of Gaussian distribution, the paracrystalline lattice factor  $Z(s)$  of the  $h$ th-order reflection is defined as

$$Z(s) = Z(h) = [1 - \exp(-4\pi^2 g^2 h^2)] / [1 - \exp(-2\pi^2 g^2 h^2)]^2 + (4 \sin^2 2\pi h) \exp(-2\pi^2 g^2 h^2)] \quad (1)$$

where  $s$  is the reciprocal lattice vector and  $g$  is the standard deviation of the Gaussian distribution divided by the average lattice vector  $\bar{a}$ . Thus, the  $g$  is a parameter to evaluate the degree of paracrystalline disorder. The integral width  $\delta\beta$  of a reflection is expressed by

$$(\delta\beta)^2 = (1/\bar{a}^2)[(1/N^2) + \pi^4 g^4 h^4] \quad (2)$$

Here,  $h$  is the scattering order and  $N$  is the number of scattering units. Figure 4a shows a plot of  $(\delta\beta)^2$  as a

function of  $h^4$  for the (110), (220), and (330) reflections of the HDPE film crystallized isothermally at  $T_c = 383$  K. The  $\delta\beta$  was the full width of the Gaussian peaks fitted to the reflections. A linear relation was obtained between the  $(\delta\beta)^2$  and  $h^4$  for both the reflections coming from the near-surface and bulk regions by the least-squares fitting method. This linear relationship was also valid for HDPE films crystallized at the other temperatures. The  $g$  and  $N$  were calculated using eq 2. Figure 4b shows the crystallization temperature dependence of  $g$  and  $N$  for the HDPE films. The  $g$  for the crystal lattice in the near-surface region of the films decreased from ca.  $3.0 \times 10^{-2}$  to  $1.7 \times 10^{-2}$  as the  $T_c$  changed from 378 to 393 K. This tendency was also observed for the  $g$  in the bulk region, but the  $g$  in the near-surface region is larger than that in the bulk region. Therefore, it was suggested that the paracrystalline distortion of the orthorhombic unit cell in the in-plane direction was larger in the near-surface region than in the bulk region. The number of the observed (110) planes,  $N$ , was ca. 50 and 52 in the near-surface and bulk regions, respectively. That is to say, the crystallite size in the in-plane direction was almost the same between the near-surface and bulk regions.

From the quantitative analysis of the GIXD data for the melt-crystallized HDPE films, it was clarified that the lattice dimension in the in-plane direction was smaller in the near-surface region than in the bulk region. Moreover, we found for the first time that the paracrystalline lattice distortion in the in-plane direction was larger in the near-surface region than in the bulk region, but the crystallite size was almost the same between these two regions. In the near-surface region, PE chains were considered to be packed closely one another to minimize the surface free energy of the films. However, chain packing was not regular there, resulting in the large lattice distortion. This might reflect the thermally unstable state of the film surface where the latent heat was released during crystallization. Another interpretation is that residual stress generated by quenching from the melt might influence paracrystalline structure in the near-surface region of melt-crystallized films. To separate the influence of residual stress from the intrinsic surface property, chain-packing structure of these films after annealing treatments should be

investigated by GIXD measurements. The structural feature at the surface of the crystalline polymers would be clarified in detail on the basis of their in-plane and out-of-plane crystallographic information. These are the subjects of our future research.

**Acknowledgment.** This research was partly supported by Fukuoka Industry, Science & Technology Foundation, and the 21st Century COE Project from The Ministry of Education, Culture, Sports, Science and Technology, Japan. The synchrotron radiation X-ray diffraction experiments were performed at SPring-8 with the approval of Japan Synchrotron Radiation Research Institute (JASRI) as Nanotechnology Support Project of The Ministry of Education, Culture, Sports, Science and Technology, Japan (Proposal 2002B0227-ND1-np/BL-13XU).

## References and Notes

- (1) Bassett, D. C. *Philos. Trans. R. Soc. London* **1994**, A348, 29–43.
- (2) Zhou, H.; Wilkes, G. L. *Polymer* **1997**, 38, 5735–5747.
- (3) Sasaki, S.; Sakaki, Y.; Takahara, A.; Kajiyama, T. *Polymer* **2002**, 43, 3441–3446.
- (4) Factor, B. J.; Russell, T. P.; Toney, M. F. *Macromolecules* **1993**, 26, 2847–2859.
- (5) Saraf, R. F.; Dimitrakopoulos, C.; Toney, M. F.; Kowalczyk, S. P. *Langmuir* **1996**, 12, 2802–2806.
- (6) Kawamoto, N.; Mori, H.; Nitta, K.; Sasaki, S.; Yui, N.; Terano, M. *Macromol. Chem. Phys.* **1998**, 199, 261–266.
- (7) Nishino, T.; Matsumoto, T.; Nakamae, K. *Polym. Eng. Sci.* **2000**, 40, 336–343.
- (8) Durell, M.; Macdonald, J. E.; Trolley, D.; Wehrum, A.; Jukes, P. C.; Jones, R. A. L.; Walker, C. J.; Brown, S. *Europhys. Lett.* **2002**, 58, 844–850.
- (9) Sakata, O.; Furukawa, Y.; Goto, S.; Mochizuki, T.; Uruga, T.; Takeshita, K.; Ohashi, H.; Ohata, T.; Matsushita, T.; Takahashi, S.; Tajiri, H.; Ishikawa, T.; Nakamura, M.; Ito, M.; Sumitani, K.; Takahashi, T.; Shimura, T.; Saito, A.; Takahashi, M. *Surf. Rev. Lett.*, in press.
- (10) Russell, T. P. *Mater. Sci. Rep.* **1990**, 5, 171–271.
- (11) Swan, P. R. *J. Polym. Sci.* **1962**, 56, 409–416.
- (12) Davis, G. T.; Eby, R. K.; Martin, G. M. *J. Appl. Phys.* **1966**, 39, 4973.
- (13) Hosemann, R. *Z. Phys.* **1950**, 128, 1–35, 465–492.
- (14) Lindenmeyer, P. H.; Hosemann, R. *J. Appl. Phys.* **1963**, 34, 42–45.
- (15) Hosemann, R.; Hindeleh, A. M. *J. Macromol. Sci., Phys.* **1995**, B34, 327–356.

MA034526Q